

A High-Speed Thermal Imaging System For Semiconductor Device Analysis

A. Hefner, D. Berning, D. Blackburn, C. Chapuy, and S. Bouché
National Institute of Standards and Technology*
Semiconductor Electronics Division
Gaithersburg, MD 20899-8124

Abstract

A new high-speed transient thermal imaging system is presented that provides the capability to measure the transient temperature distributions on the surface of a semiconductor chip with 1- μ s time, and 15- μ m spatial resolution. The system uses virtual instrument graphical user interface software that controls an infrared thermal microscope, translation stages, digitizing oscilloscope, and a device test fixture temperature controller. The computer interface consists of a front panel for viewing the temperature distribution and includes a movie play-back feature that enables viewing of the temperature distribution versus time. The computer user interface also has a sub-panel for emissivity mapping and calibration of the infrared detector. The utility of the system is demonstrated in this paper using a bipolar transistor hotspot current constriction process.

I. Introduction

Many semiconductor device failure mechanisms involve non-uniform heating of the semiconductor chip surface for dynamic fault conditions [1,2]. A high-speed thermal imaging capability is needed to analyze the rapidly changing temperature distributions in the study of these failure mechanisms. In addition, high-speed transient thermal imaging is needed to measure the shape of small heat sources because the heat from these small sources rapidly diffuses to surrounding areas masking the original heat source shape and location. Because present commercial infrared imaging systems provide limited transient thermal imaging capability, it is the purpose of this paper to present a new system that enables for the first time the precise measurement of high speed transient thermal images.

Several commercial instruments are available that provide the ability to analyze the steady-state temperature distribution on the semiconductor chip surface using either a large area infrared detector with an oscillating mirror to raster the image, or an infrared imaging device where the image is obtained by an array of pixels on the detector. The systems based upon thermal imaging arrays are limited in speed. The single pixel large-area detectors, on the other hand, have the ability to obtain a measurable electronic signal for high-speed transient events but only in a single spot "stare" mode where the mirror rastering is not used. Furthermore, the signal-to-noise ratio for the high-speed signals is not sufficient for temperatures near 25 °C, an important operating range for semiconductor devices. The high-gain detector amplifiers used to obtain a

measurable signal also result in substantial drifting of the signal reference over a one-second time frame.

In ref. [3], an averaging and signal referencing technique was developed to improve the precision and calibration of high-speed temperature waveform measurements. In the present paper, this high-speed temperature measurement technique is extended to scan the full image of the semiconductor chip surface, producing a movie of the high-speed transient event. The new system successively acquires the temperature waveform at each coordinate of the sample using the technique developed in ref. [3], and uses an XY-coordinate translation stage to step between coordinates. This technique requires a repetitive heating event that can be cycled at a sufficient rate so that the averaging and scanning can be completed in a reasonable time, and so that the transient thermal distribution can be acquired before any degradation occurs within the sample. Potentially destructive fault conditions can be examined with this technique by terminating the fault condition just before the destruction condition is reached at each cycle of the repetitive event, as shown in the example of Section III.

II. Test System Description

A sophisticated computer instrument control and high-level user interface is required to facilitate the many scanning, translation, and calibration functions required for the new high-speed thermal imaging system developed in this work. The measurement system requires control of the test fixture temperature, acquisition of the detector voltage waveforms from a digitizing oscilloscope, translation of the temperature controlled test fixture to the different X and Y positions, and calculation of temperature from the detector voltage at each time and position. In addition, the emissivity calibration procedure requires waveform calculations to establish the relationship between the detector output voltage and the surface temperature of the sample on a point by point basis.

The LabWindows/CVI** virtual instrument development software is used to develop the new measurement system. LabWindows/CVI is a C-programming language development platform that provides the capability to develop an interactive graphical computer user interface that controls instruments through the IEEE-488 instrumentation bus. The equipment used for the new system described in this paper includes a Barnes Engineering Computherm III infrared microscope, a

* Contribution of the National Institute of Standards and Technology; not subject to copyright.

** LabWindows/CVI™ is a trademark of National Instruments Inc. Certain commercial products or materials have been identified in order to specify or describe the subject matter of this paper adequately. This does not imply recommendation or endorsement by the National Institute of Standards and Technology, nor does it imply that the products are the best for the purpose.

Tektronix TDS 754D digitizing oscilloscope, a JC Systems Inc. temperature controller, and a Newport MM3000 XY-coordinate motion controller. The LabWindows/CVI software development platform also provides math analysis libraries and direct C-programming language capability required for the data analysis.

A. Virtual Instrument User Interface Front Panel

Figure 1 shows the user interface front panel for the high-speed thermal imaging system. The panel consists of various pull down menus, buttons, and data entry/display fields used to operate the measurement system. The pull-down menus on the top menu bar are used to load and save data and calibration files as well as to print results. The buttons, graphs, and data fields within the window are used to control the data-acquisition and result-analysis process. The process used to calibrate the instrument and sample emissivity is described in Subsection II-B, and an example of the use of the system to analyze a bipolar transistor hotspot is given in Section III.

The items in the box in the upper left-hand quadrant of Fig. 1 are used to obtain a temperature waveform for a single position, to set up the instrument and waveform parameters to be used at each position of a thermal scan, and to display the temperature waveform of selected positions after a position-dependent measurement has been made. The buttons in the middle of the left hand side are used to set the origin for the motion control and to set and read the test fixture temperature. The buttons in the box on the bottom left-hand side are used to define the region and increment size to be scanned by the motion controllers and to initiate the thermal image measurement. Finally, the displays and controls on the right-hand side are used to display the thermal image results after the measurements are completed.

Because the high-gain detector-amplifier signal has an offset that drifts with times on the order of one second, the temperature values must be calculated relative to a reference within the high-speed transient waveform. This is

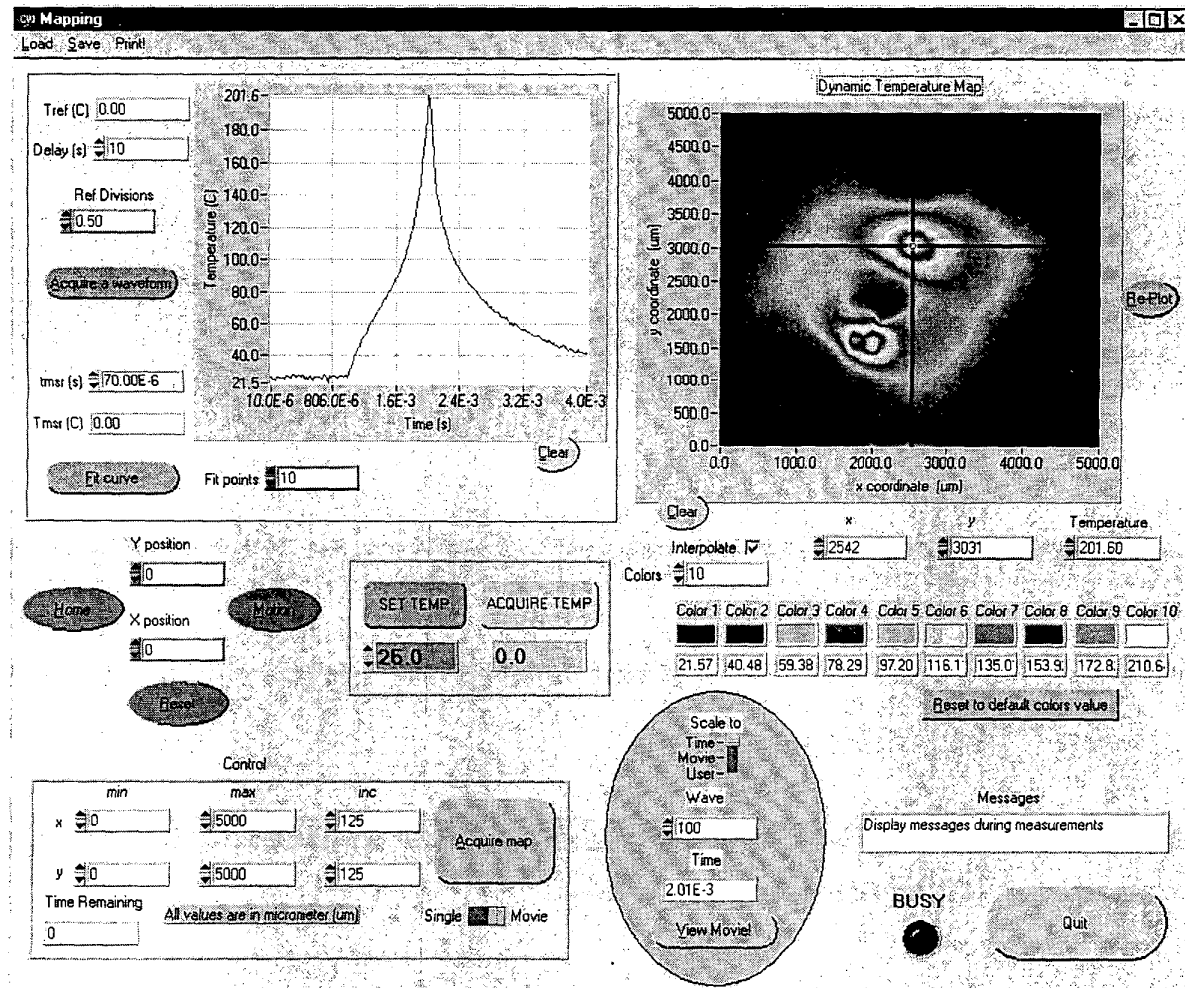


Figure 1. Virtual instrument user interface front panel for the high-speed thermal imaging system.

accomplished using the left-hand portion of the transient waveform where the temperature controller determines the reference temperature before the transient heating pulse begins. The value used by the program for the reference temperature is displayed in the data entry field labeled " T_{ref} ." This value can be entered manually or is obtained from the temperature controller when the "Acquire TEMP" button is pressed. The program determines the detector voltage at the reference temperature by averaging all of the data points in the first number of divisions displayed in the data entry field labeled "Ref Divisions" (the default value shown is 0.5 divisions). The temperature waveform shown in the upper left-hand graph of Fig. 1 is calculated as described in Section II-B. The graph also has a cursor that can be moved along the waveform with the mouse to display the values of time and temperature in the display fields " t_{msr} " and " T_{msr} ," respectively.

To perform the position-dependent measurements, the stage movement buttons in the middle of the left-hand side of Fig. 1 are used to set the origin for the motion control. The data entry fields within the box on the lower left-hand side are then used to set the ranges and increments for the

scan positions. When the "Acquire map" button is pushed, the transient thermal image measurement begins and the "Time Remaining" to complete the measurement is continually updated. When the measurement is completed, the program will have retained the temperature data for each scan position and time increment.

The results of the transient thermal image measurement are analyzed using the controls and displays on the right-hand half of Fig. 1. The contour plot in the upper right-hand corner of Fig. 1 displays the temperature distribution on the sample surface at a given time or during a movie playback. The cross-hair cursor on the contour plot is used to select the position for the temperature waveform on the upper left-hand graph and for the numeric readouts just below the contour plot.

The temperatures and colors of the counters are displayed in the boxes labeled "Color 1" through "Color 10." Each color can be changed by right clicking the mouse on the color box, and the numeric values for the contours can be changed if "Scale to User" is selected within the oval-shaped region. The contours can also be automatically

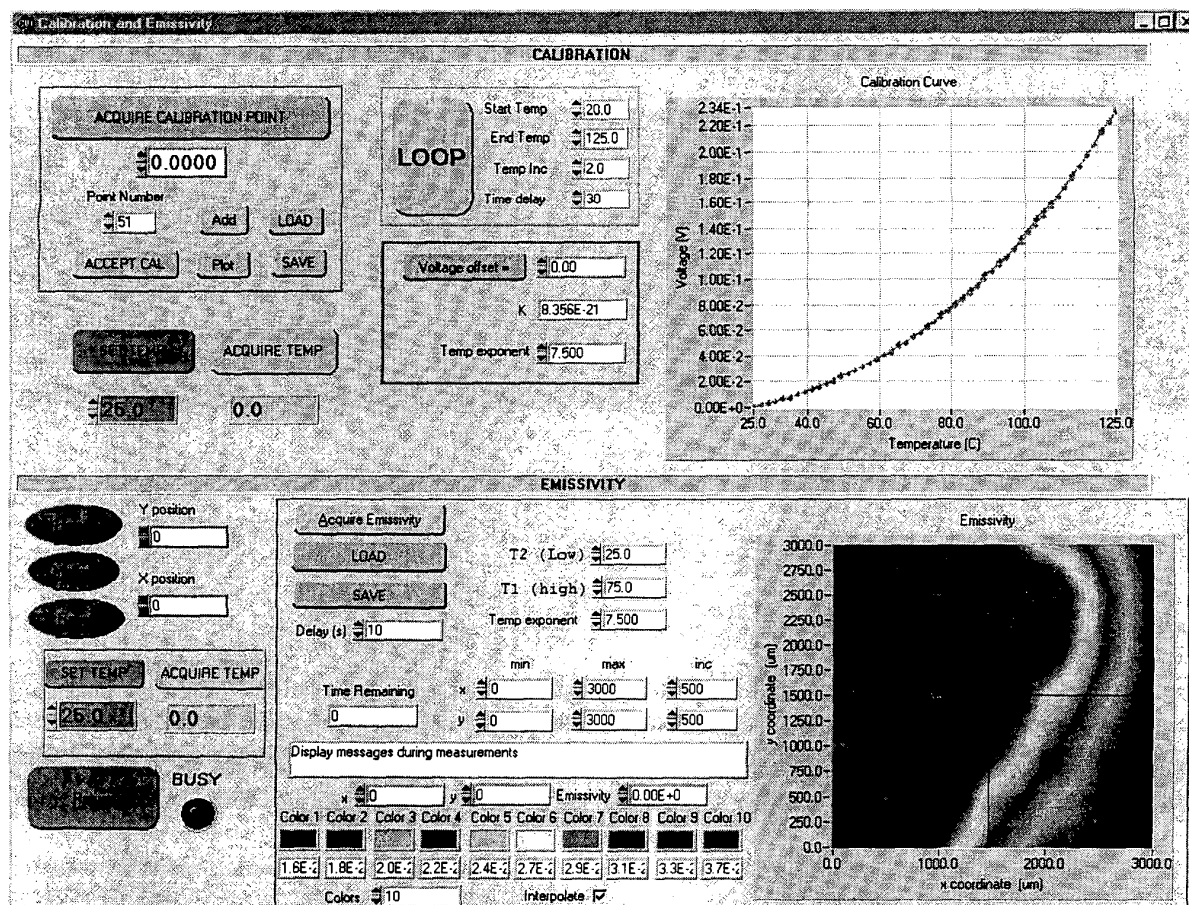


Figure 2. User interface sub-panel for calibration and emissivity mapping.

scaled to the temperature range of each frame if the "Scale to Time" is selected or scaled to the temperature range of the entire movie if the "Scale to Movie" is selected. The "View Movie" button is used to view the entire movie or each frame of the movie can be selected by entering the value in the "Wave" data entry box where the time of the frame is displayed in the display field labeled "Time."

B. Emissivity and Detector Calibration Sub-Panel

Before measurements can be made from the user interface panel of Fig. 1, it is necessary to calibrate the response of the measurement system detector and amplifier, and the emissivity versus position of the sample surface. Figure 2 shows the calibration and emissivity sub-panel. The calibration data for the detector and amplifier, and emissivity temperature coefficient can be measured using the upper half of the panel, or can be loaded from a pre-existing file using the "LOAD" button. The data and fitted curve in the upper right-hand graph is an example of the calibration of the temperature dependence of detector voltage. The calibration of the emissivity versus position on the sample is obtained using the lower half of the sub-panel of Fig. 2. The contour plot in the lower right-hand side of Fig. 2 is an example of an emissivity map of the corner of an aluminum-covered chip (left-hand side) on top of a copper header (right-hand side).

The data in Fig. 2 are obtained using a double-differential method where the reference is provided using a chopper wheel placed between the sample and the infrared microscope detector. This differential method is required because the offset of the high gain detector amplifier drifts with time on the order of one second. To obtain the calibration data, the oscilloscope is set up to measure the square-wave voltage signal obtained from the detector amplifier measuring the radiance of a temperature-controlled sample through the chopper wheel. Each data point is taken for a single position of the sample surface with the detector operating in the stare mode.

The "Acquire Calibration Point" button in the upper left-hand box of Fig. 2 acquires the waveform from the oscilloscope, automatically detects and averages the upper and lower levels of the square wave, and calculates the differential signal voltage of the sample referenced to the chopper blade. The other buttons in the upper left-hand box are then used to accept the data point, or load and save the calibration curves. The parameters in the box containing the "LOOP" button can be used to sequentially obtain a series on calibration data where the program sets the temperature of the test fixture, monitors until the set temperature is reached, and then acquires the calibration point at each temperature.

Figure 3 illustrates the measured square wave and the portions of the waveform averaged to determine the detector voltage due to the radiance of the sample (V_s) and the voltage due to the radiance of the chopper blade (V_c). The differential detector voltage is defined as

$$\Delta V = V_s - V_c. \quad (1)$$

After a sequence of calibration data is obtained, the "Voltage offset" button is used to reference the calibration

curve to $\sim 25^\circ\text{C}$, thus eliminating the chopper blade radiance as a variable:

$$V = \Delta V(T) - \Delta V(25^\circ\text{C}) = V_s(T) - V_s(25^\circ\text{C}). \quad (2)$$

This function also calculates the values of the constants "K" and the temperature exponent " α " using a least squares fit of the data to the equation:

$$V = K \cdot T^\alpha. \quad (3)$$

The measured calibration data in the upper right-hand graph of Fig. 2 fits this expression well over the entire range where the device can be externally heated. Because the pulsed chip surface temperatures can be higher than the melting temperature of the die-attach solder, this expression also provides the extrapolation capability for pulsed heating conditions.

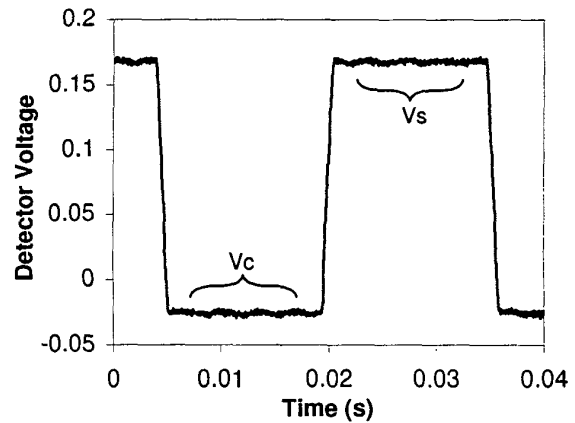


Figure 3. Measured square wave detector voltage signal indicating regions averaged to determine detector voltage due to radiance of $1\ \mu\text{s}$ sample (V_s) and radiance of chopper blade (V_c).

The value of K in eq 3 includes the detector and amplifier gain and local emissivity of the sample. The value of α includes the temperature dependence of blackbody radiation and the temperature dependence of the sample emissivity. Assuming that the temperature dependence of emissivity is independent of position on the sample, only the value of K is needed for each position on the sample to obtain the emissivity map in the lower right-hand contour graph of Fig. 2. Alternatively, the temperature-dependent curve could be measured for each position of the sample, but this would require substantially more time for the calibration.

To obtain the value of K versus position, the differential radiance voltage is thus measured at each position for two different temperatures to eliminate the voltage due to the radiance of the chopper blade. Similarly to eq 1, the differential voltages for the two temperatures are defined as:

$$\Delta V(T_1) = V_s(T_1) - V_c \quad (4a)$$

$$\Delta V(T_2) = V_s(T_2) - V_c. \quad (4b)$$

Subtracting these two equations and using eq 2 results in

$$\Delta V(T_1) - \Delta V(T_2) = V(T_1) - V(T_2) \quad (5)$$

Finally, using the expression for $V(T)$ given in eq 3 results in an expression for K in terms of the two temperature values and the differential voltages:

$$K = (\Delta V(T_1) - \Delta V(T_2)) / (T_1^\alpha - T_2^\alpha) \quad (6)$$

This expression is used to calculate the value of K at each point in the sample based upon the measured differential voltage at the two temperatures.

To acquire the data needed for the emissivity map, the values of T_1 and T_2 as well as the range and increment values for the X and Y coordinates are entered into the fields within the box on the lower half of Fig. 2. When the "Acquire Emissivity" button is pushed, the program sets the test fixture temperature to T_1 , acquires the T_1 radiance data for each position on the sample surface, and then repeats the measurements for temperature T_2 . The program then calculates the emissivity map of the sample using eq 6. The "Return" button on Fig. 2 is used to return to the user interface front panel of Fig. 1 to measure temperature waveforms and transient thermal images using the calibration data.

As described in Subsection II-A, the temperature waveform of each position is calculated by referencing the detector voltage waveform to the voltage of the left-hand side of the waveform that corresponds to the reference temperature. Using eq 3, the reference temperature voltage is calculated as

$$V_{ref} = K T_{ref}^\alpha \quad (7)$$

and temperature waveform is calculated using

$$T(t) = ((V(t) - V_{ref}) / K)^{1/\alpha} \quad (8)$$

III. Application Example

Several application examples were studied to determine the speed and utility of the new measurement system. The speed was examined by applying a well-defined, 10 μ s constant power dissipation pulse to a power MOSFET. The observed temperature waveforms indicated the expected linear adiabatic temperature rise demonstrating the 1 μ s time resolution. The utility of the high-speed transient thermal measurement system for studying rapidly changing temperature distributions is demonstrated in this paper using a bipolar transistor hotspot current constriction process.

Considerable effort has been previously dedicated to the measurement and understanding of power transistor forward biased Safe Operating Area (SOA) limits. Moreover, the thermal instabilities that result in power device hotspot formation have been studied in detail. Power bipolar transistor hotspot formation occurs for a specific range of voltage (high voltage) and current (low current), resulting in a rapid rise in junction temperature (more than 150 $^{\circ}$ C), and the transition

from relatively uniform current conduction to extremely nonuniform conduction. If the power pulse is extended after the formation of a dynamic hotspot, the hotspot will reach the destruction temperature and the transistor will be degraded or destroyed.

The conditions of the experiment have to be set such that a hotspot is just beginning to form but has not progressed to the point of destroying the device. The hotspot occurs for high voltages on the limit of thermal instability. Several experiments were performed to determine the condition where the hotspot is beginning to form. The conditions presented in this paper that result in hotspot formation but not destruction are: $V_{CE}=265$ V, $I_C=0.5$ A, pulse width of 1 ms, and ambient temperature of 25 $^{\circ}$ C. The repetition rate is chosen to be less than 100 Hz so that the sample cools to the controlled fixture temperature before each cycle begins, thus providing a reference at the beginning of the temperature waveform.

The transient thermal images acquired for this condition show that the increase in temperature is nonuniform and that the current constricts to a small region of the transistor. The electrical signature for hotspot formation is also observed (sudden drop in base-emitter voltage at device terminals) for this same condition [1]. Figure 4 shows several frames from the movie that indicate the formation of the dynamic hotspot. Figure 4a shows the temperature distribution before the hotspot begins to form; 4b is at the onset of hotspot formation, 4c is at the end of the heating pulse where the peak temperature occurs, and 4d is during the cooling phase where the heat begins to spread. The contour graphs of Fig. 4 were plotted with the "Scale to Time" setting to demonstrate that the heat is focused within the hotspot for Fig. 4c.

Note that for the "Scale to Time" setting, the color contour definitions are changed with each image. If the "Scale to Movie" setting is used, all image frames in the movie sequence use the same contour color definitions. The former setting emphasizes the change in temperature distribution between frames and the latter emphasizes the change in temperature magnitude between frames.

Figure 5 shows the transient temperature waveforms defined by using the cross hair cursor within the contour plot. Figure 5a corresponds to the point where the hotspot is formed, and Fig. 5b to a point that is not within the hotspot. The temperature waveforms initially start with the 25 $^{\circ}$ C test fixture temperature. When the power pulse is applied (at approximately the 1 ms point in Fig. 5) the temperature first begins to rise nearly linearly due to uniform, nearly adiabatic heating for the constant power pulse. Both curves reach 60 $^{\circ}$ C at nearly the same time (at approximately the 1.6 ms point). Once the hotspot begins to form, the temperature at the point of the hotspot then begins to make a rapid curvature toward higher temperatures. In the regions of the device where the hotspot is not formed, the temperature does not curve upward. Although the heating was initially uniform, the maximum temperature of the hotspot is 220 $^{\circ}$ C and the rest of the chip only reaches 82 $^{\circ}$ C. The heating pulse is terminated at approximately the 2 ms point and the temperature begins to fall.

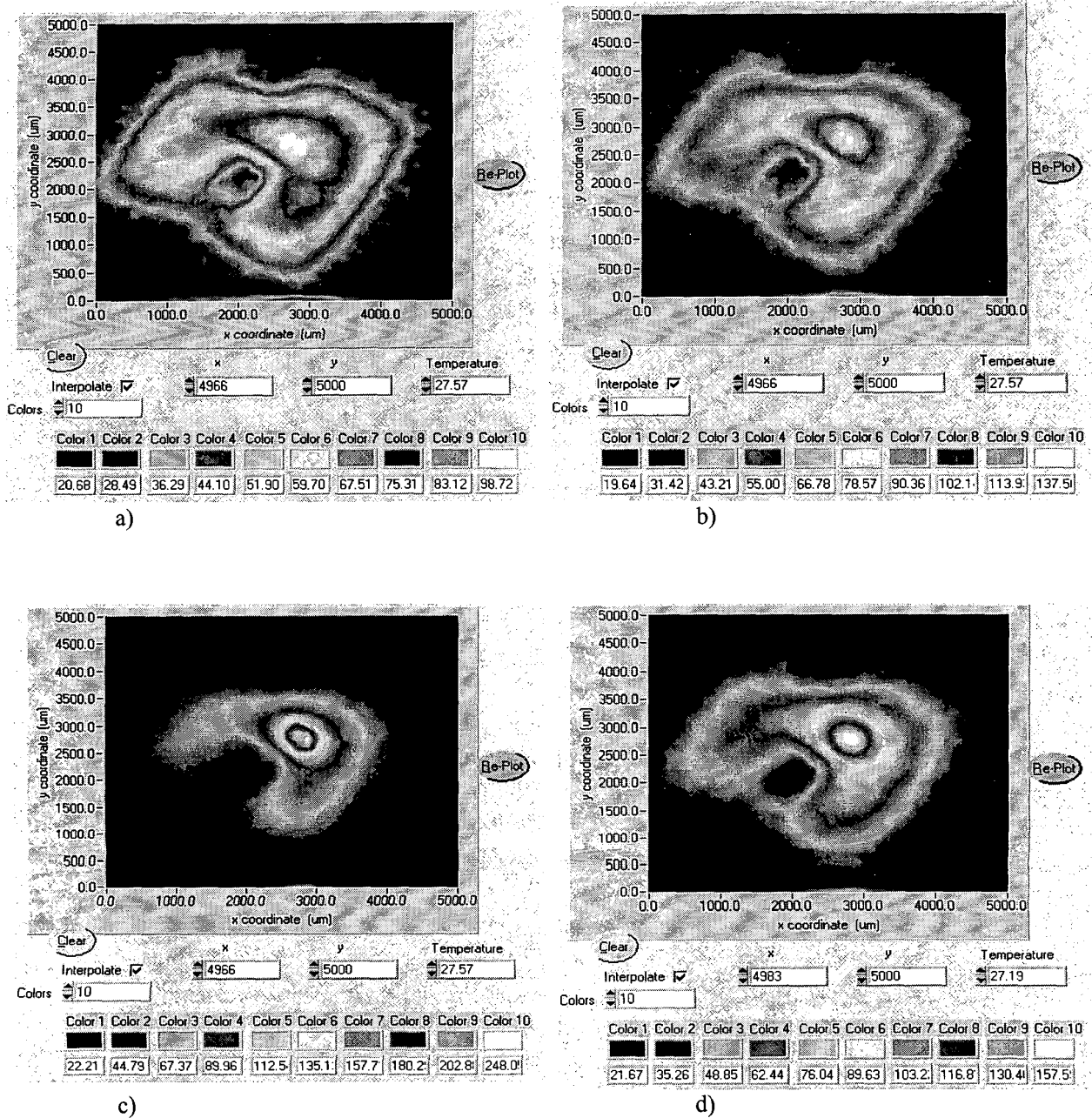


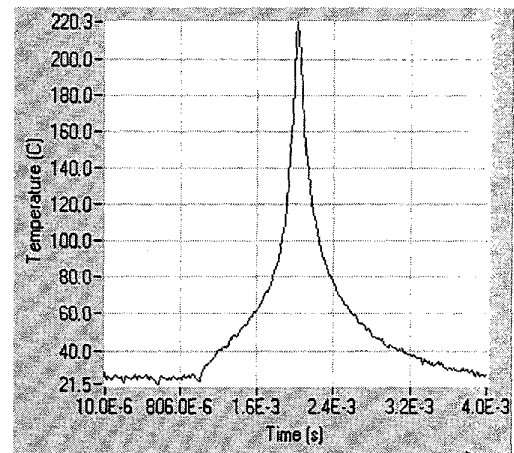
Figure 4. Temperature distribution a) before the hotspot begins to form, b) at the onset of hotspot formation, c) at the end of the heating pulse where the peak temperature occurs, and d) during the cooling phase where the heat begins to spread.

IV. Conclusion

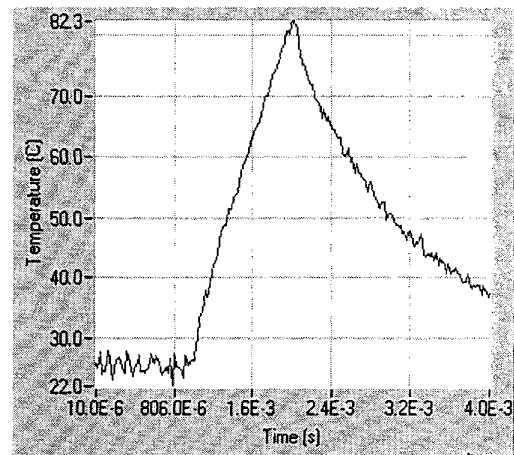
A new high-speed transient thermal imaging system is developed that provides the capability to measure the transient temperature distributions on the surface of a semiconductor chip with 1 μ s time, and 15 μ m spatial resolution. The system uses virtual instrument graphical user interface software that controls an infrared thermal microscope, translation stages, digitizing oscilloscope, and a device test fixture temperature controller. The new system is several orders of magnitude faster than conventional infrared thermal imaging systems. The higher speed enables the observation of semiconductor device dynamic failure events and enables the localization of small heat sources before the heat has time to diffuse to surrounding areas.

References

- [1] Hower, Blackburn, Oettinger, and Rubin, "Stable Hotspots and Second Breakdown in Power Transistors," Power Electronics Specialists Conference Record, pp. 234-246 (1976).
- [2] Consoli, Gennaro, Testa, Consentino, Frisna, Letor, and Magri, "Thermal Instability of Low Voltage Power MOSFETS" IEEE Trans. On Power Electronics, vol. 15, pp. 575-581 (May 2000).
- [3] Hefner and Blackburn, "Thermal Component Models for Electro-Thermal Network Simulation," IEEE Trans. Components, Packaging, and Manufacturing Technology, vol. 17, p. 413 (1994).



a)



b)

Figure 5. Transient temperature waveforms for a) the point where the hotspot is formed, and b) a point that is not within the hotspot.



COLOR

Your accompanying CD-ROM contains a
version of this paper with color images.
<http://www.cpmi.org/proceedings/order.html>